Developmental Biology **231,** 334–347 (2001)
doi:10.1006/dbio.2000.0148, available online at http://www.idealibrary.com on IDEAL®

Connexin31-Deficiency in Mice Causes Transient Placental Dysmorphogenesis but Does Not Impair Hearing and Skin Differentiation

Achim Plum,*,[1] Elke Winterhager,† Joerg Pesch,‡ Juergen Lautermann,§ Gaby Hallas,* Boris Rosentreter,* Otto Traub,* Claus Herberhold,‡ and Klaus Willecke*,[2]

**Institut für Genetik, Universität Bonn, Römerstr. 164, Bonn D-53117, Germany; ‡Klinik und Poliklinik für Hals-Nasen-Ohrenkranke, Sigmund-Freud-Str. 25, Bonn D-53105, Germany; †Institut für Anatomie, Universitätsklinikum Essen, Hufelandstrasse 55, Essen D-45122, Germany; and §HNO-Klinik, Universitätsklinikum Essen, Hufelandstrasse 55, Essen D-45122, Germany*

Mutations in the human *GJB3* gene that codes for Connexin31 (Cx31), a protein subunit of gap junction channels, have recently been reported to cause deafness and the skin disorder *erythrokeratodermia variabilis.* To study the function of this gene in mice, we generated animals with targeted replacement of the Cx31 gene (*Gjb3*) by a *lacZ* reporter gene. Although homozygous Cx31-deficient adult mice ($Gjb3^{-/-}$) were found among the offspring of heterozygous Cx31-deficient parents ($Gjb3^{+/-}$), 60% of the animals expected according to Mendelian inheritance were lost between ED 10.5 and 13.5. Placentas of $Gjb3^{-/-}$ embryos at ED 9.5 were smaller than controls as a result of severely reduced labyrinth and spongiotrophoblast size. From ED 10.5 onward, placentas of surviving $Gjb3^{-/-}$ embryos recovered progressively and reached normal size and morphology by ED 18.5. This corresponds to a time period in which another connexin isoform, Connexin43, is upregulated in spongiotrophoblast cells of Cx31-deficient and control placentas. No morphological or functional defects of skin or inner ear were observed in surviving adult $Gjb3^{-/-}$ mice. We conclude that Cx31 is essential for early placentation but can be compensated for by other connexins in the embryo proper and adult mouse.

Key Words: **gap junctions; gene targeting; Connexin31; *Gjb3;* placenta; inner ear.**

INTRODUCTION

Connexins are the protein subunits of gap junction channels, which allow the direct exchange of ions, metabolites, and second messengers up to a molecular mass of 1000 Da between the cytoplasmic compartments of contacting cells. These proteins can assemble into homomeric or heteromeric hemichannels that dock to hemichannels of the same or different connexin composition in the plasma membrane of neighboring cells to form functional homotypic or heterotypic channels, respectively (Elfgang *et al.*, 1995). Connexins are encoded by a family of at least 15 genes in rodents (cf. Goodenough *et al.*, 1996; Manthey *et al.*, 1999). Connexin proteins differ in their pattern of expression and biophysical properties of the channels to which they contribute.

Connexin 31 (Cx31) is an exceptional member of this gene family. It is one of the earliest connexin proteins expressed in murine development and is present in the compacted morula and throughout the blastocyst (Reuss *et al.*, 1996; Dahl *et al.*, 1996). After implantation, its expression becomes restricted to the ectoplacental cone and its derivatives (Reuss *et al.*, 1996; Dahl *et al.*, 1996). In rat Cx31 expression correlated with the proliferative phase of the trophoblast (Reuss *et al.*, 1996). In the mouse embryo proper Cx31 is markedly expressed in the presumptive rhombomeres r3 and r5, showing a striking overlap with the

[1] Present address: mice & more GmbH & Co. KG, Martinistr. 52, Hamburg D-20251, Germany.

[2] To whom correspondence should be addressed at Universität Bonn, Institut für Genetik, Abteilung Molekulargenetik, Römerstr. 164, Bonn D-53117, Germany. Fax: 49-228-734-263. E-mail: genetik@uni-bonn.de.

0012-1606/01 $35.00

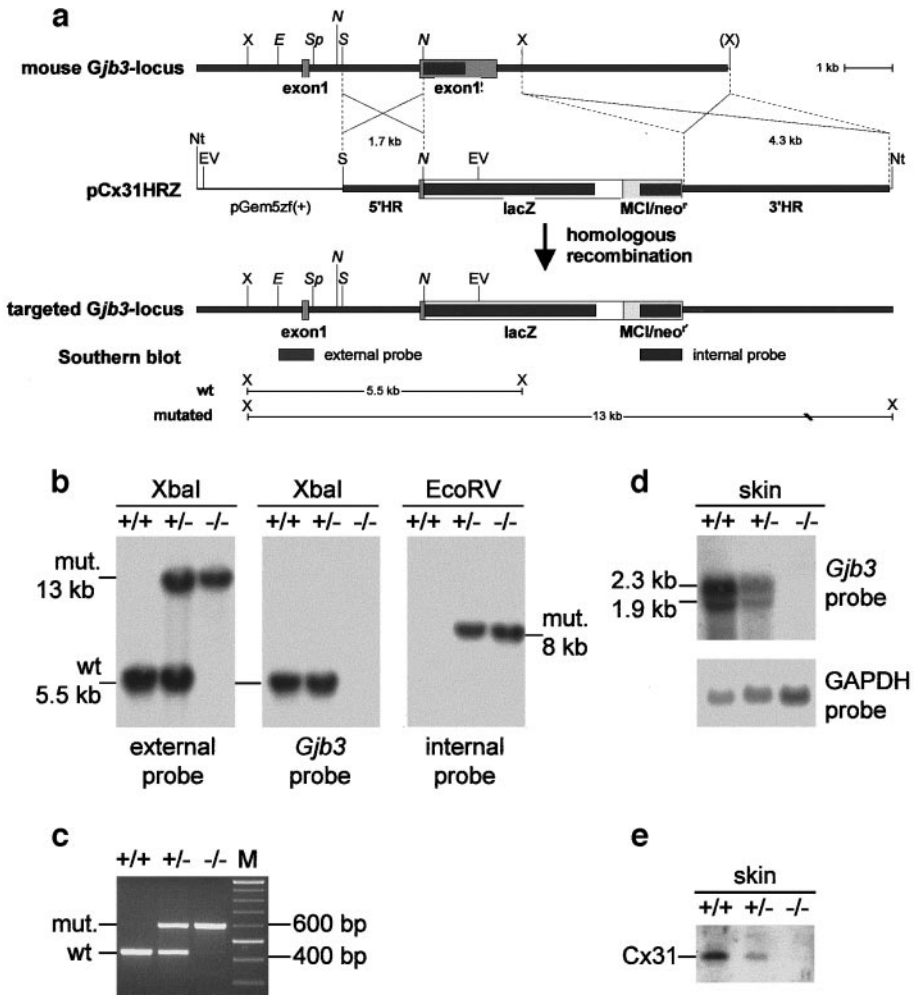

FIG. 1. Generation of Cx31-deficient mice. (a) For homologous recombination in embryonic stem cells a targeting vector (pCx31HRZ) was used that contained a total of 6 kb of DNA homologous to the *Gjb3* locus. A region of 1895 bp, including the whole Cx31-coding region downstream of the start codon, was replaced by a promoterless *lacZ* reporter gene (*lacZ*) without nuclear localization signal followed by neomycin resistance gene under control of the MCI promoter (*MCI/neo*^{r}), both followed by a polyadenylation signal. Successful homologous recombination was detected by Southern blot hybridization of *Xba*I (X)-digested genomic DNA using an *Eco*RI (E)/*Spe*I (Sp) fragment located upstream of the 5′ homology region (5′HR) as a probe. Absence of further random vector integrations was assessed by probing *Eco*RV (EV)-digested DNA with an internal probe homologous to the *neo*^{r} coding region. (b) Viable *Gjb3*$^{-/-}$ mice were found among the offspring of *Gjb3*$^{+/-}$ parents as proven by Southern blot analysis. Only the 13-kb *Xba*I fragment, indicative of the mutated allele, was detected using the external probe, while hybridization with the Cx31-coding region and the internal probe confirmed the absence of the wild type allele and the presence of mutated allele in these mice. (c) To detect the wild type and the mutant allele in DNA from tail biopsies and embryo preparations, a PCR strategy was developed using primers specific for the Cx31-coding region and the *lacZ* reporter gene, respectively, in conjunction with an anchor primer, binding in the upstream intron of *Gjb3*. (d) Northern blot analysis of total RNA extracted from back skin confirmed the reduction or absence of Cx31 transcripts in *Gjb3*$^{+/-}$ and *Gjb3*$^{-/-}$ mice, respectively. The blot was hybridized with the Cx31-coding region, stripped, and reprobed with glycerolaldehyde-3-phosphate dehydrogenase-specific probe (GAPDH) for normalization. (e) Cx31 deficiency in *Gjb3*$^{+/-}$ and *Gjb3*$^{-/-}$ mice was further confirmed by Western blot analysis of total skin protein. E, *Eco*RI; EV, *Eco*RV; N, *Nco*I; Nt, *Not*I; S, *Sma*I; Sp, *Spe*I; X, *Xba*I; HR, homology region; wt, wild type; M, molecular weight standard; mut., mutated; GAPDH, glycerolaldehyde-3-phosphate dehydrogenase.

expression of *krox-20* (Dahl *et al.*, 1997), a key regulator of hindbrain segmentation (Schneider-Maunoury *et al.*, 1993). In adult mice Cx31 is observed in suprabasal skin and testis. The distinct regulation of Cx31 expression in development and the finding that Cx31 hemichannels show only homotypic coupling (Elfgang *et al.*, 1995) prompted speculations that Cx31 is involved in the formation of developmental compartments (Dahl *et al.*, 1996). Recently, different domi-

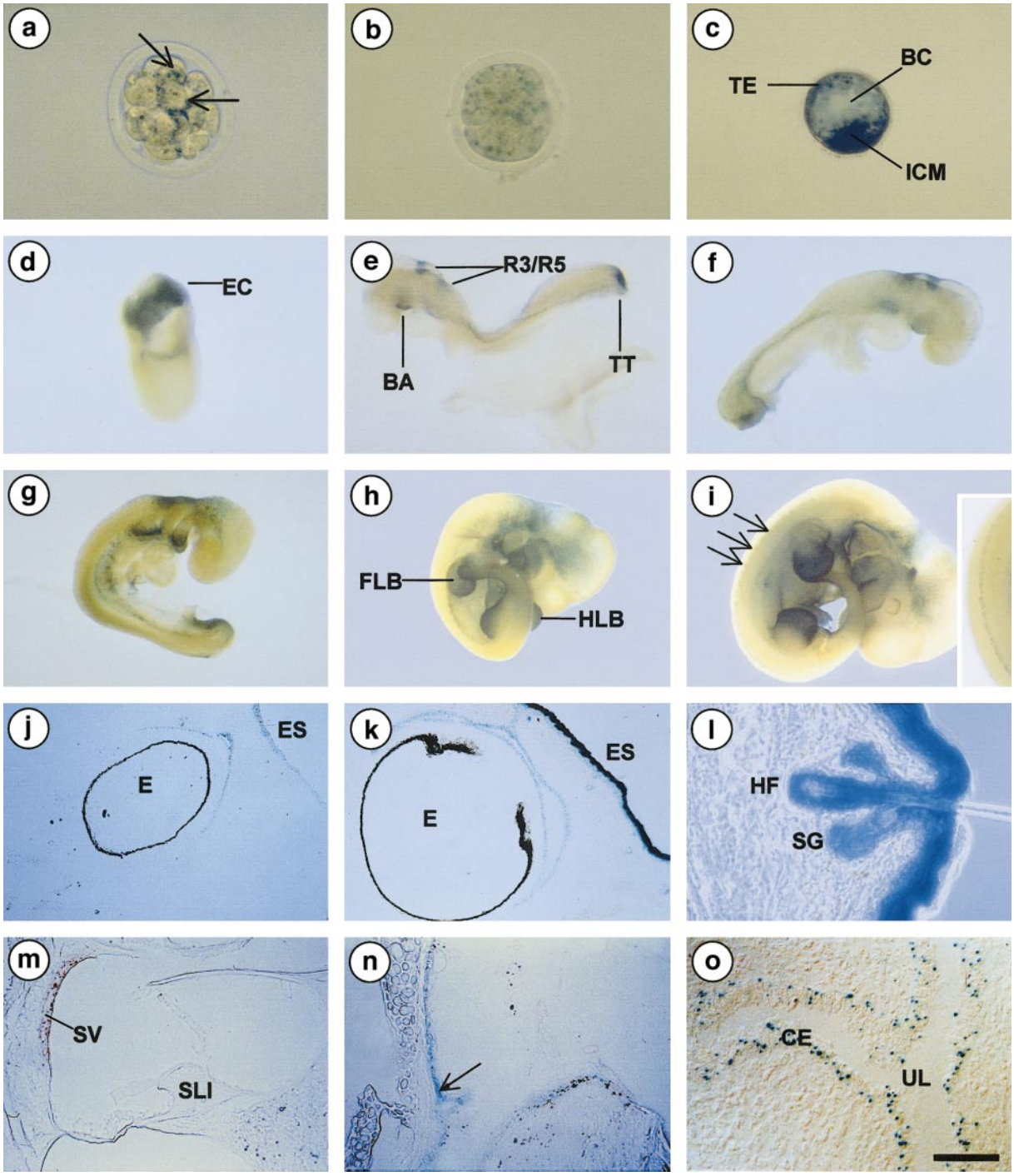

FIG. 2. Temporal and spatial regulation of Cx31 expression analyzed by staining for cytoplasmic *lacZ* reporter gene expression in *Gjb3*$^{+/-}$ embryos and tissue sections. Corresponding *Gjb3*$^{+/+}$ samples were stained in parallel as negative controls (not shown). Whole mount stainings of uncompacted morula (a), compacted morula (b), blastocyst (c), and postimplantation embryos around ED 7.5 (d), ED 8.25 (e), ED 8.75 (f), ED 9.5 (g), ED 10.5 (h), and ED 11.5 (i). While only sparse staining was detected in uncompacted morulae (arrows in (a)) expression spreads over all blastomeres after compaction (b) and strongly increases during the development of the blastocyst (c), where staining was equally strong in trophectoderm (TE) and inner cell mass (ICM). In postimplantation development expression was found in the ectoplacental cone at ED 7.5 (d), rhombomeres 3 and 5 (R3/R4), branchial arches (BA), and tail tip (TT) starting from ED 8.25 (e–i). From ED 10.5 onward (h), a distal-to-proximal gradient of expression was observed in front and hind limb buds (FLB, HLB). At ED 11.5 a metameric staining lateral to the dorsal midline appeared, indicating expression in the dorsal root ganglia [arrows and box in (i)]. Staining

nant mutations in the human Cx31 gene (*GJB3*) have been suggested to cause two inherited disorders, *erythrokeratodermia variabilis*, a skin disease (Richard *et al.*, 1998a), and high-frequency hearing impairment (Xia *et al.*, 1998). However, the molecular mechanism by which different mutations in the same connexin gene can cause different diseases is presently not understood (Steel, 1998). Recently, mutations in human *GJB3* have also been associated with recessive nonsyndromic deafness (Liu *et al.*, 2000).

Although these observations suggest an important role of Cx31 in human skin differentiation and hearing, we found that Cx31-deficient mice did not show any phenotypic alterations of epidermis or auditory function. However, 60% of the homozygously mutated embryos died between embryonic day (ED) 10.5 and ED 13.5. This was accompanied by transient placental dysmorphogenesis. Our analyses of connexin expression in the placenta suggest that the upcoming expression of another placental connexin, Connexin43 (Cx43), can rescue some of the homozygously Cx31-deficient embryos.

MATERIALS AND METHODS

Generation of Mice

A fragment of genomic 129/Sv mouse DNA spanning about 20 kb of the *Gjb3* locus was isolated from λDashII library (Stratagene, La Jolla, CA) using mouse *Gjb3* cDNA as a probe (Hennemann *et al.*, 1992). As 5′ homologous region, a 1.7-kb *Sma*I/*Nco*I fragment including the *Gjb3* start codon was inserted into an in-frame *Sma*I site at the beginning of the promoterless *lacZ* gene of the vector pLRlacZpAMCIneopA (a generous gift of Dr. Frank Sablitzky, London, UK), while a 4.3-kb *Xba*I fragment was inserted into an *Spe*I site downstream of the neomycin^r gene (*neo*^{r}) in the backbone. The resulting targeting construct pCx31HRZ contained 6 kb of DNA homologous to the *Gjb3* locus, in which all of the Cx31-coding region downstream of the start codon and the 3′UTR had been replaced by the *lacZ* reporter gene and the *neo*^{r} gene under control of the *MCI* promoter.

R1 ES cells (Nagy *et al.*, 1993) were transfected with vector DNA, linearized downstream of the 3′ homologous region by *Not*I and selected for stable integration by 350 μg/ml G418, and subcloned as described by Hogan *et al.* (1994). Resistant clones were analyzed for homologous recombination at the *Gjb3* locus by Southern blot hybridization. Correctly recombined clones were injected into C57BL/6 blastocysts that were transferred into pseudopregnant foster mothers as described by Hogan *et al.* (1994). Chimeras were checked for germ line transmission of the mutated allele by crossing to C57BL/6 mice. Heterozygous offspring were once more backcrossed with C57BL/6 mice, before *Gjb3*$^{+/-}$ mice were intercrossed, to obtain homozygously mutated progeny. Thus, all experiments were carried out on a mixed genetic background with an average of 75% C57BL/6 and 25% 129. Mice were kept under standard housing conditions with a 12-h light/12-h dark cycle with food and water *ad libitum*. All experiments were carried out in accordance with German law for animal protection and with permission of the state.

Genotyping of ES Cells and Mouse Tissues

Correct targeting in ES cells and transgenic mice was confirmed by Southern blotting of *Xba*I-digested genomic DNA probe with an *Eco*RI/*Spe*I fragment spanning the first exon of *Gjb3*, which recognized a 5.5- and a 13-kb fragment representing the wild type and the mutated allele, respectively. Absence of the Cx31-coding region in the mutated alleles was confirmed by stripping and rehybridizing the blot with a probe homologous to the deleted region. Additional random integrations of the vector were excluded by Southern blotting of *Eco*RV-digested DNA, probed with an internal probe homologous to the *neo*^{r} cassette. For routine genotype analysis, tail tips, whole embryos (ED 2.5–ED 8.5), or extraembryonic membranes (ED 9.5–ED 18.5) were lysed at 55°C in PCR buffer (10 mM Tris–Cl, pH 9, 50 mM KCl, 0.1% Triton X-100) containing proteinase K (120 μg/ml). Lysates were cleared by brief centrifugation and an aliquot was subjected to PCR using the primers Cx31GT1 (*Gjb3* intron; sense; ctg gac tct gac atg tgc aca tac), Cx31GT2 (Cx31-coding region; antisense; cta cat gca gga tga cca gca tag), and Cx31GT3 (*lacZ*-coding region; antisense; cca cag atg aaa cgc cga gtt aac), and *Taq* DNA polymerase (Promega, Madison, WI). *Gjb3* wild type and mutated allele could be distinguished by the sizes of the resulting product.

Northern Blot Hybridization

Total RNA was extracted using TRIZOL (Gibco BRL, Karlsruhe, Germany) according to manufacturer's instructions. Back skin was freed of bulk hair using scissors before preparation. A minimum of three placentas were pooled per time point and genotype. RNA was size fractionated, blotted, and hybridized as described (Hennemann *et al.*, 1992). [^{32}P]-labeled fragments spanning the coding regions of the Cx26-, Cx31-, and Cx43-encoding genes were used as probes. Loads were normalized by reprobing the blots using a [^{32}P]-end-labeled $(dT)_{17}$-oligonucleotide (Ausubel *et al.*, 1989) or a glyceraldehyde-3-phosphate dehydrogenase (GAPDH) probe, followed by densitometric quantification using the VDS-Imagemaster software (Pharmacia, Freiburg i. Br., Germany).

---

of tissue sections through embryo heads in the area of the eyes (E) at ED 13.5 (j) and ED 17.5 (k) and adult skin with hair follicle (l) indicated an epidermal *lacZ* expression that started around ED 13.5 in embryonic skin (ES) and increased during further development to adult skin where additional expression was observed in hair follicles (HF) and sebaceous glands (SG). No specific staining was detected in the cochlea neurosensory epithelium, the stria vascularis (SV), the spiral ligament, and the spiral limbus (SLI) (m). The epithelial lining of the middle mucosa adjacent to the cochlea served as positive control (arrow in n). In the uterus (o) a faint staining was observed in the ciliary epithelium (CE) lining the uterine lumen (UL). Bar: a–c, 70 μm; d, 80 μm; e, f, 400 μm; g, 600 μm; h, i, 1000 μm; j, k, 480 μm; l, 120 μm; m, 170 μm; n, 80 μM; o, 40 μm.

Western Blot Analysis

Preparation and Western blot analysis of total skin protein, using polyclonal rabbit antibodies specific for Cx31, were carried out as described previously by Butterweck *et al.* (1994).

LacZ Staining

Embryos of up to ED 11.5 were stained as whole mounts, while adult tissues and embryos beyond ED 12.5 were first sectioned (10–20 μm) on a cryostat and transferred onto superfrost plus slides (Menzel, Brunswick, Germany). Fixing and staining was essentially carried out as described by Hogan *et al.* (1994). In brief, the material was fixed with 0.2% glutaraldehyde in 0.1 M phosphate buffer (pH 7.3) containing 2 mM $MgCl_2$ and 5 mM EGTA (ethyleneglycol-bis-(2-aminoethyl)-tetraacetate), rinsed three times in 0.1 M phosphate buffer (pH 7.3) containing 2 mM $MgCl_2$, 0.01% sodium doxycholate, and 0.02% Nonidet P-40 (N 6507 Sigma, Deisenhofen, Germany) and stained in the same solution supplemented with 1 mg/ml X-gal (5-bromo-4-chloro-3-indolyl-β-D-galactopyranoside), 5 mM potassium ferricyanide, and 5 mM potassium ferrocyanide at 37°C for 12–24 h. Sections were then mounted in Aquatex (Merck, Darmstadt, Germany), while whole-mount preparations were stored in 70% ethanol.

Histological Analyses

For morphological analyses, placentas from embryos between ED 6.5 and ED 18.5, adult skin, testis, and inner ear were fixed in 3.7% formaldehyde in phosphate-buffered saline (PBS) for a minimum of 48 h at 4°C, dehydrated, and embedded in paraffin. Sections (3 μm) were dried overnight, deparaffinized with xylene, hydrated through a graded series of ethanol, stained with azan or hematoxylin/eosin, dehydrated, cleared in xylene, and mounted in Entellan (Merck).

Immunohistochemistry

For cryostat sections, placentas were immediately frozen in liquid nitrogen and kept at −80°C. For staining of Cx26 (Traub *et al.*, 1989), Cx31 (Butterweck *et al.*, 1994), and Cx43 (Traub *et al.*, 1994) cryostat sections were processed routinely. Briefly, sections were fixed for 10 min in 96% ethanol and, after rinsing with PBS, covered with 1% bovine serum albumin solution (BSA; Sigma) to block nonspecific binding sites. Incubation with the primary antibody for 1 h was followed by the appropriate secondary FITC-conjugated antibody for 45 min. Sections were covered with Vectashield (Vector Laboratories, Peterborough, UK) and analyzed using an Axiophot fluorescence microscope (Zeiss, Oberkochen, Germany). Immunostaining of inner ear was carried out as described previously (Lautermann *et al.*, 1998) using antibodies directed to Cx26 (Traub *et al.*, 1989), Cx30 (Kunzelmann *et al.*, 1999), and Cx31 (Butterweck *et al.*, 1994).

For double immunostaining, the polyclonal rabbit antibody against Cx31 (see above) was used first, followed by the appropriate Cy3-conjugated secondary antibody (Dianova, Hamburg, Germany). Then the sections were incubated with a polyclonal antibody against Cx43 raised in the goat (Santa Cruz Biotechnology, Santa Cruz, CA) followed by an FITC-conjugated anti-goat antibody (Dako, Hamburg, Germany). Sections were examined using a confocal laser-scanning microscope (LSM 510; Zeiss) in a dual-channel scanning mode.

Proliferation

A minimum of three placentas per time point and genotype were analyzed. Samples were fixed, embedded, sectioned (7 μm), deparaffinized, and rehydrated as described for histological analyses. After incubation of endogenous peroxidases by 5-min incubation with 3% (v/v) H_2O_2 in PBS, sections were treated with PCNA-specific monoclonal antibodies (Dako) in PBS for 30 min at room temperature and rinsed three times with PBS. Subsequently, sections were incubated with biotin-linked secondary antibodies (1:50 in PBS; 30 min; 20°C; Dako), washed three times in PBS, and incubated with streptavidin-coupled peroxidase (1:50 in PBS; 30 min; 20°C, Dako). After three washes in PBS, peroxidase was detected by 5-min incubation with 3′-diaminobenzidine-tetrahydrochloride (DAB; Dako). Sections were rinsed in distilled water, dehydrated through a graded series of ethanol, cleared in xylene, and mounted in Entellan (Merck).

Audiometry

Auditory response threshold was measured by means of electrical response audiometry (ERA) using tone pips with center frequencies of 2, 4, 8, 16, and 32 kHz. A standard clinical system (Multiliner; Jaeger & Toennies, Hoechberg, Germany) was used for registration and averaging of 800 single sweeps for each frequency and sound pressure level (SPL). Low-frequency tone pips (2–4 kHz) were applied using standard headphones (DT48; Beyerdynamic, Heilbronn, Germany) of the recording system, while high-frequency tone pips (8–32 kHz) were presented using a piezoelectrical speaker (PH8; Visatone, Haan, Düesseldorf, Germany) driven by an external function generator (PM59193; Philips, Amsterdam, The Netherlands) in conjunction with a dB-attenuator (Hewlett–Packard, Palo Alto, CA). Mice were anesthetized by intraperitoneal injection of thiopental (60 μg/g body weight in PBS) and placed 40 mm in front of the speaker in a soundproof box. Three silver needle electrodes were placed subcutaneously in a symmetrical array just rostral to the pinna so that electrode impedance was below 5 kOhms. The electrode placed ipsilateral to the speaker was used as active electrode, while the middle electrode was used as a reference and the contralateral as a ground. Brain-stem responses were recorded for each frequency starting at 100 dB SPL and subsequently decreased in 10-dB increments until no auditory response could be detected in the averaged sweeps. SPLs were corrected for distance between speaker and ear by calibration with a sound level meter (Type 2235; Brüel & Kjaer, Harrow, Great Britain). Initially two age groups of 6 and 12 months of $Gjb3^{+/+}$ and $Gjb3^{-/-}$ mice were measured, but data were later pooled according to genotypes because no differences were detected between the different age groups. Auditory thresholds were plotted as average ± SEM against frequency in logarithmic scale.

Statistical Analysis

Data are presented as means ± SD. A one-way ANOVA and post hoc Tukey B tests were used for comparison of placental weights at different time points. Probability values of $P < 0.05$ were considered significant.

RESULTS

Generation of Mice

Cx31-deficient mice were generated using a targeting construct in which the whole Cx31-coding region immedi-

TABLE 1

Genotypes Obtained after Matings of Heterozygous Cx31-Deficient Mice

			Genotypes					
			Gjb3$^{+/+}$		*Gjb3*$^{+/-}$		*Gjb3*$^{-/-}$	
Stage	$N_{litters}$	$N_{animals}$	N	%	N	%	N	%
−3.5 dpc[a]	6	116[b]	22	19.0	63	54.3	31	26.7
9.5 dpc	10	88	30	34.1	35	39.8	23	26.1
11.5 dpc	8	49	18	36.7	19	38.8	12	24.5
15.5 dpc	7	56	20	35.7	26	46.4	10	17.9
16.5 dpc	6	47	17	36.2	24	51.0	6	12.8
>21 dpp[a]	26	168	48	28.6	103	61.3	17	10.1

[a] dpc, days postcoitum; dpp, days postpartum.
[b] Mothers were superovulated.

ately downstream of the start codon was replaced by a promotorless *lacZ* reporter gene without nuclear localization signal and a neomycin resistance gene (*neo*^{r}) under control of the *MCI* promotor (Fig. 1a). After transfection and G418 selection, nine out of 192 resistant embryonic stem cell clones showed homologous recombination at the *Gjb3* locus, giving a frequency of 4.7%. After injection into blastocysts, one clone gave rise to chimeras that transmitted the mutated allele through the germ line. Interbreeding of heterozygous Cx31-deficient mice (*Gjb3*$^{+/-}$) resulted in viable homozygous Cx31-deficient mice (*Gjb3*$^{-/-}$) as proven by Southern, PCR, Northern, and Western blot analyses (Figs. 1b–1e).

LacZ Reporter Gene Expression in Heterozygous Cx31-Deficient Mice

Stainings for cytoplasmic *lacZ* reporter gene activity in *Gjb3*$^{+/-}$ mice confirmed the expression pattern previously observed using other methods (Hennemann *et al.,* 1992; Butterweck *et al.,* 1994; Dahl *et al.,* 1996, 1997; Davies *et al.,* 1996). Thus, staining was first seen during embryogenesis in the compacted morula and the blastocyst (Figs. 2a–2c). By ED 7.5 *lacZ* expression became restricted to the ectoplacental cone (Fig. 2d) and was first observed in the embryo proper in rhombomeres r3 and r5 just before turning (ED 8.25) and in branchial arches and tail tip (Figs. 2e and 2f). Rhombomere staining remained high until ED 9.5 and gradually decreased thereafter (Figs. 2f–2i). In addition, a previously not described, distal-to-proximal gradient of expression in the outgrowing limb buds was observed from ED 10.5 onward (Figs. 2h and 2i). At ED 11.5, a metameric pattern lateral-to-dorsal midline appeared, indicating Cx31 expression in the dorsal root ganglia (ED 11.5; Fig. 2i). Expression of *lacZ* did not differ between *Gjb3*$^{+/-}$ and

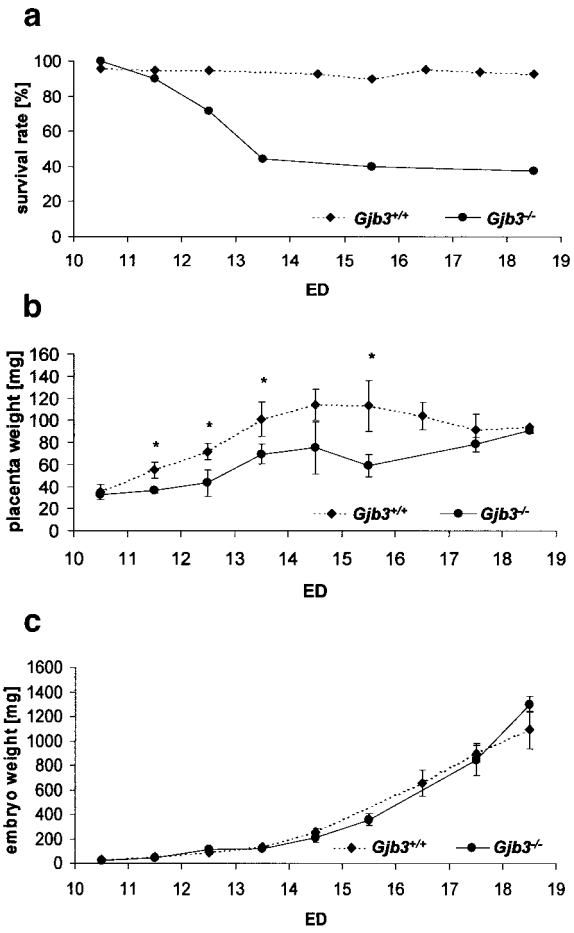

FIG. 3. Embryo survival and growth between ED 10.5 and ED 18.5. (a) Embryonic survival after mating of *Gjb3*$^{-/-}$ parents compared to *Gjb3*$^{+/+}$ parents of the same genetic background monitored as the ratio of living embryos (i.e., embryos with visible heart beat) to implantation chambers. Weight of placentas (b) and embryos (c) after mating of *Gjb3*$^{+/+}$ and *Gjb3*$^{-/-}$ parents, respectively. Wet samples were weighed after excess of fluid was drained. A minimum of 14 samples were analyzed per time point. All weights are given as means ± SD. Asterisks indicate time points where values differed significantly ($P < 0.05$) between *Gjb3*$^{+/+}$ and *Gjb3*$^{-/-}$ animals. ED, embryonic day.

TABLE 2

Parental Genotype and Litter Size at Birth

Parental genotype			
Father	Mother	$N_{litters}$	$N_{pubs}/N_{litters}$ (means ± SD)
Gjb3$^{+/+}$	*Gjb3*$^{+/+}$	10	7.0 ± 1.5
Gjb3$^{+/+}$	*Gjb3*$^{-/-}$	8	7.1 ± 1.0
Gjb3$^{-/-}$	*Gjb3*$^{+/+}$	9	7.3 ± 1.6
Gjb3$^{+/-}$	*Gjb3*$^{+/-}$	27	6.6 ± 2.2
Gjb3$^{-/-}$	*Gjb3*$^{-/-}$	10	3.0 ± 1.3

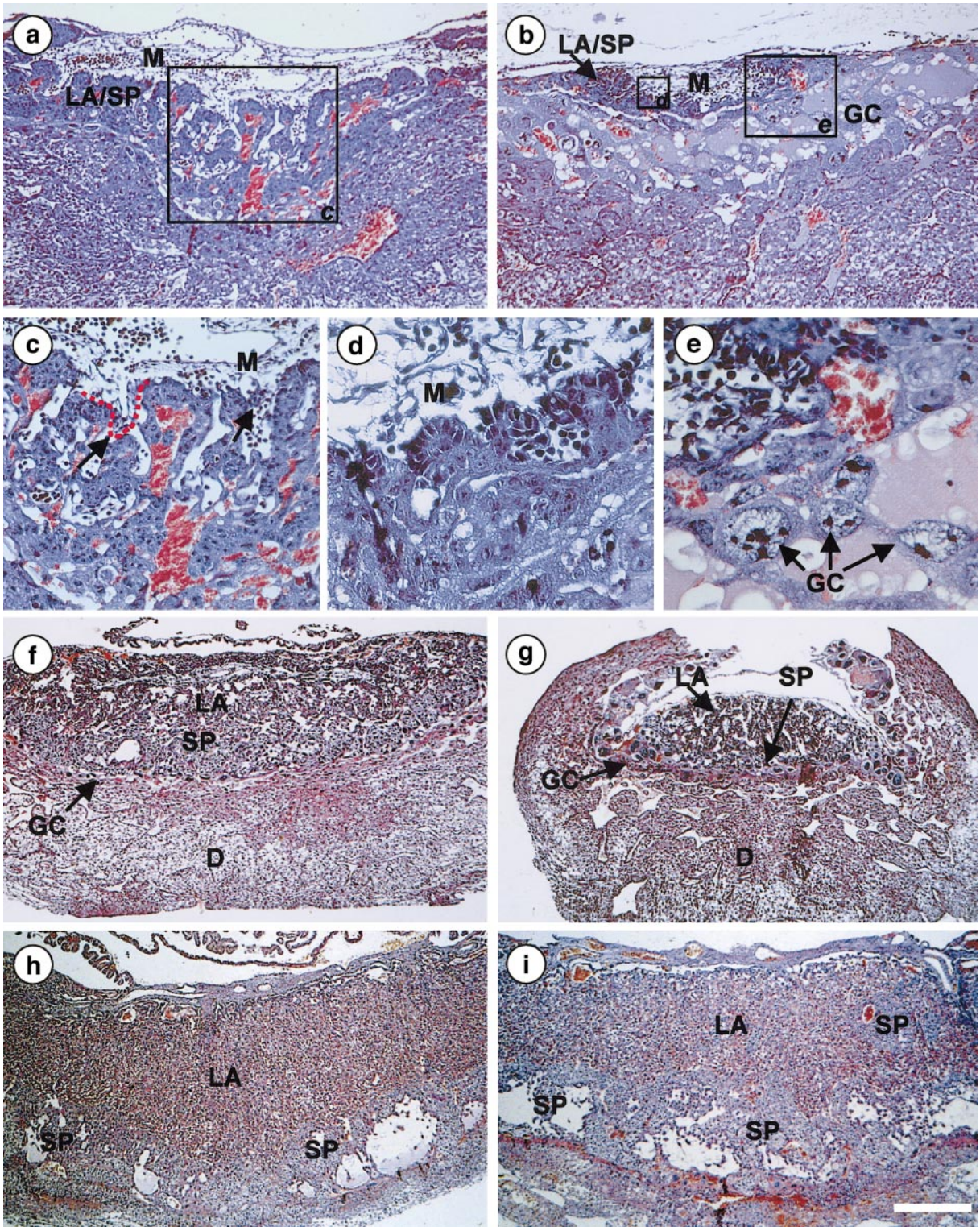

FIG. 4. Transient placental dysmorphogenesis in Cx31-deficient embryos. Azan-stained paraffin sections of wild type and Cx31-deficient placentas. Overview of $Gjb3^{+/+}$ (a) and $Gjb3^{-/-}$ (b) placentas at ED 9.5. Panels (c)–(e) show higher magnifications of the boxed areas in (a) and (b) as indicated in the boxes. Overview of $Gjb3^{+/+}$ (f, h) and $Gjb3^{-/-}$ (g, i) placentas at ED 12.5 (f, g) and ED 14.5 (h, i). Fingerlike protrusions of maternal mesenchyme in wild type placenta at ED 9.5 are indicated by arrows and a dotted line in (c). M, allantoic mesenchyme; LA, labyrinth; SP, spongiotrophoblast; D, decidua; GC, giant cells. Bar: 470 μm in (a, b; f–i).

Gjb3$^{-/-}$ embryos between ED 8.0 and ED 11.5. In skin *lacZ* expression was first detected at ED 13.5, increased progressively until ED 17.5, and persisted in suprabasal layers, hair follicles, and sebaceous glands of adult epidermis (Figs. 2j–2l). While Cx31 protein was previously detected only in the granular layers (Butterweck *et al.*, 1994), β-galactosidase was also found in the cornified layers of epidermis, possibly reflecting the greater stability of the bacterial enzyme. *LacZ* expression in testis was weak and could not be attributed unequivocally to a specific cell type. In the uterus, a faint staining was observed throughout the menstrual cycle in the ciliary epithelium of the endometrium (Fig. 2o). No expression of *lacZ* was observed in the adult inner ear of *Gjb3*$^{+/-}$ and *Gjb3*$^{-/-}$ mice, but some staining was found in the epithelium of the semicircular ducts (Figs. 2m and 2n).

Decreased Embryonic Survival and Placental Dysmorphogenesis

Despite the birth of viable *Gjb3*$^{-/-}$ mice, statistical analysis of litters after crossings of *Gjb3*$^{+/-}$ mice revealed that only about 40% of the *Gjb3*$^{-/-}$ animals, expected for Mendelian inheritance, survived to the age of weaning (Table 1: 10.1% vs 25%). The remaining homozygous animals were lost after ED 11.5. Similar crossing of *Gjb3*$^{-/-}$ mice resulted in strongly reduced litter sizes, a phenomenon that was solely dependent on the embryos' genotype, because matings of *Gjb3*$^{-/-}$ mice of either sex with *Gjb3*$^{+/+}$ mice of the opposite sex resulted in normal litters sizes (Table 2). Monitoring the number of implantation chambers and living embryos (i.e., embryos with beating hearts) revealed that 60% of these embryos were lost between ED 10.5 and ED 13.5 (Fig. 3a). This was accompanied by a reduction in size and weight of the placenta of *Gjb3*$^{-/-}$ embryos, which only reached the weight of control placentas at ED 18.5 (Fig. 3b). Although embryos appeared more heterogeneous in size between ED 10.5 and ED 13.5, average weight of living *Gjb3*$^{-/-}$ embryos did not differ significantly from that of controls (Fig. 3c). Histological analysis of implantation chambers, starting at ED 6.5, showed that early placental development was unaffected (data not shown). However, between ED 8.5 and ED 9.5, *Gjb3*$^{-/-}$ placentas were smaller than control placentas (Figs. 4a and 4b). The labyrinthine part was barely developed and the chorionic plate consisted of only some loosely arranged stem cells. Maternal lacunas filled with blood between the spongiotrophoblast and labyrinth layers were less frequent. The allantoic mesenchyme, including the embryonic blood vessels, lacked the typical fingerlike protrusions into the labyrinth. While spongiotrophoblast cells were sparse, large numbers of trophoblastic giant cells were found at the border of the maternal decidual tissue (Figs. 4c–4e). Chorio-allantoic fusion was not affected.

From ED 10.5 onward the placenta recovered. Labyrinth development progressed and a small spongy layer was formed, although maternal and embryonic areas were still separated by a large number of giant cells (Figs. 4f and 4g). From ED 14.5 onward, no obvious difference apart from reduced size and a slightly disorganized appearance of the labyrinth and spongiotrophoblast layers could be observed in *Gjb3*$^{-/-}$ placentas (Figs. 4h and 4i). This transient dysmorphogenesis was accompanied by a delayed proliferative activity in *Gjb3*$^{-/-}$ placentas. While at ED 9.5 proliferation was high in the labyrinth and spongiotrophoblast of *Gjb3*$^{+/+}$ placenta, almost no proliferation was observed in *Gjb3*$^{-/-}$ placentas (Figs. 5a and 5b). At ED 12.5, in contrast, proliferation in *Gjb3*$^{+/+}$ placentas was sparse, while almost all cells and cell types proliferated in *Gjb3*$^{-/-}$ placentas (Figs. 5c and 5d). Northern blot analysis of Cx26-, Cx31-, and Cx43-mRNA expression in total placenta between ED 10.5 and ED 18.5 revealed that, while Cx31 transcript levels went up slightly with ongoing development, Cx43 transcripts increased fourfold, and Cx26-mRNA abundance decreased to background levels during the same period (Fig. 6). Immunofluorescence analysis revealed that Cx43 protein was not detected in the trophoblast before ED 10.5. Between ED 10.5 and ED 18.5 Cx31 and Cx43 protein was found in spongiotrophoblast cells (Figs. 7a, 7b, 7e, and 7f) and, in accordance with Northern blot data, levels of Cx43 protein increased markedly, while levels of Cx31 remained roughly unchanged. Furthermore, Cx43 protein was detected in giant cells at ED 18.5 (Figs. 7c and 7d). Cx26 protein was found in the labyrinthine part as previously described (Figs. 7g and 7h). Although Cx43-mRNA levels increased earlier in *Gjb3*$^{-/-}$ placentas, no qualitative or quantitative difference could be observed in immunolocalization and immunoreactivity for Cx26 and Cx43, when compared to those of controls (data not shown).

The colocalization of Cx43 and Cx31 in spongiotrophoblast cells was further confirmed by double immunostaining for both connexin isoforms in sections of ED 12.5 placentas in combination with laser-scanning microscopy. This revealed that both connexins are not only expressed in the same cells but also seem to localize in the same gap junction plaque (Fig. 8).

No obvious defects were observed in *Gjb3*$^{-/-}$ embryos around the time of embryo loss. Thus, in contrast to *krox-20*$^{-/-}$ mice (Schneider-Maunoury *et al.*, 1993), pattern formation of the hindbrain was unaffected in *Gjb3*$^{-/-}$ embryos at ED 11.0, as judged by the relative position of ganglia deriving from rhombomeres r2 and r4 (data not shown).

Normal Epidermis, Testis, and Inner Ear of Adult Cx31-Deficient Mice

Surviving adult *Gjb3*$^{-/-}$ mice did not differ in outward appearance, weight, or fertility from their wild type (*Gjb3*$^{+/+}$) littermates. Histological comparison of skin (i.e., the tissue with the strongest expression of Cx31 in adult mice) did not reveal any obvious phenotypic alterations in *Gjb3*$^{-/-}$ mice (Figs. 9a and 9b). Neither site nor strength of expression of various marker proteins for epidermal differentiation, namely keratins 2e, -6, -10, -14, and α6-integrin

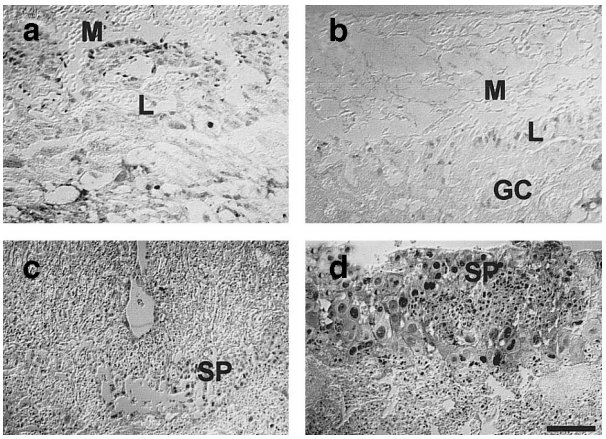

FIG. 5. Cell proliferation in wild type and Cx31-deficient placenta. Paraffin sections of *Gjb3*$^{+/+}$ (a, c) and *Gjb3*$^{-/-}$ (b, d) placentas at ED 9.5 (a, b) and ED 12.5 (c, d) stained for PCNA. M, mesenchyme; L, labyrith; SP, spongiotrophoblast; GC, giant cells. Bar: 235 μm.

(cf. Moll *et al.*, 1982; Sonnenberg *et al.*, 1991), differed between *Gjb3*$^{-/-}$ an *Gjb3*$^{+/+}$ mice (data not shown). Despite the expression of Cx31 in testis (Hennemann *et al.*, 1992) an endometrium of the uterus (Fig. 2o), breeding performance and litter size of *Gjb3*$^{-/-}$ males and females (Table 2) did not hint to any functional impairment of reproduction. Testis size and histology did not differ from that of controls (Figs. 9c and 9d).

Mutations in the Cx31 gene (*GJB3*) were reported to be causal to premature high-frequency hearing impairment (Xia *et al.*, 1998) and recessive nonsyndromic deafness (Liu *et al.*, 2000) in humans. However, in adult *Gjb3*$^{-/-}$ mice, auditory thresholds between 2 and 32 kHz measured by recording of evoked brain-stem potentials were not increased when compared to those of wild type mice of the same age (6 and 12 months) and genetic background (Fig. 10). Moreover, histological analyses of adult Cx31-deficient inner ear did not yield any obvious phenotypic alterations (Figs. 9e and 9f). In accordance with *lacZ* stainings (Figs. 2m and 2n), immunofluorescent analysis of consecutive sections of inner ear of adult *Gjb3*$^{+/+}$ and *Gjb3*$^{-/-}$ mice did not reveal any signals specific for Cx31, whereas Cx30 and Cx26 were readily detected in all cells of the spiral limbus, fibrocytes of the spiral ligament, and basal cells of the stria vascularis (data not shown). Cx26 and Cx30 expression did not differ between *Gjb3*$^{+/+}$ and *Gjb3*$^{-/-}$ mice (data not shown).

DISCUSSION

Here we show that Cx31 is essential for early placental development, but dispensable in the embryo proper and adult mice.

Using various rat trophoblast-derived cell lines, Grummer *et al.* (1996) and Winterhager *et al.* (1996) could positively correlate Cx31 expression with trophoblast proliferation but not with differentiation. By deleting the Cx31-coding region we showed in this study that Cx31 is necessary for normal spongiotrophoblast growth and differentiation in mice. Upon implantation the polar trophectoderm of the blastocyst, which is in contact with the inner cell mass, proliferates and differentiates into chorion and

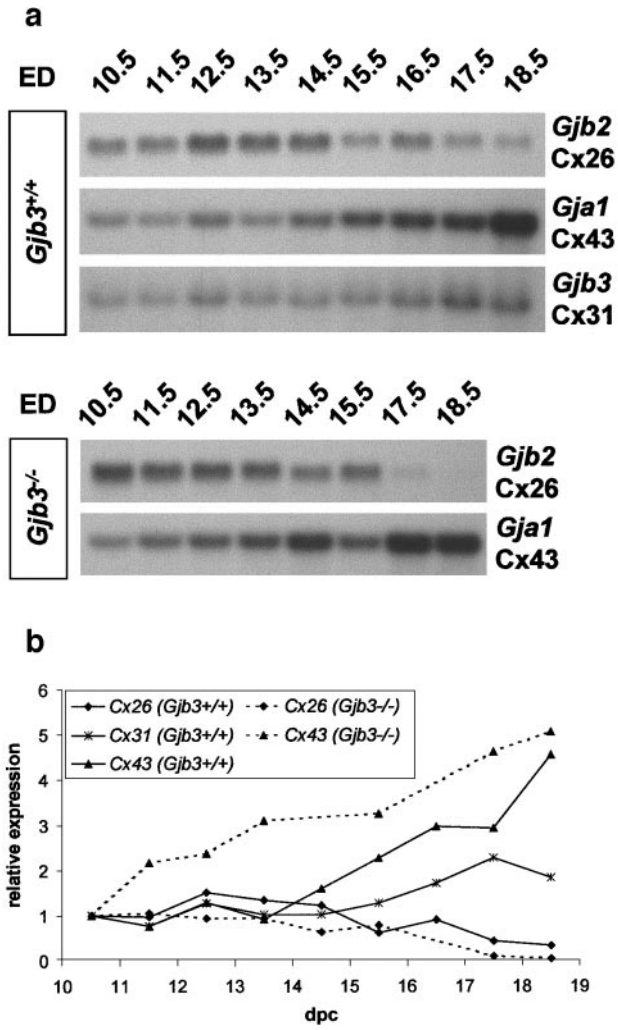

FIG. 6. Connexin expression in placenta between ED 10.5 and 18.5. (a) Northern blot hybridization of total RNA of *Gjb3*$^{+/+}$ and *Gjb3*$^{-/-}$ placentas using probes homologous to the coding regions of the Cx26-, Cx31-, and Cx43-encoding genes (*gjb2*, *Gjb3*, and *gja1*, respectively). For each time point a minimum of three placentas were pooled. (b) Densitometric evaluation of the autoradiographs shown in (a). Signals were normalized for loading differences by rehybridization of the blots to an oligo(dT) probe and plotted with reference to the signal obtained from wild type placentas at ED 10.5. The genotype of the embryos from which the placentas were obtained is given in parentheses.

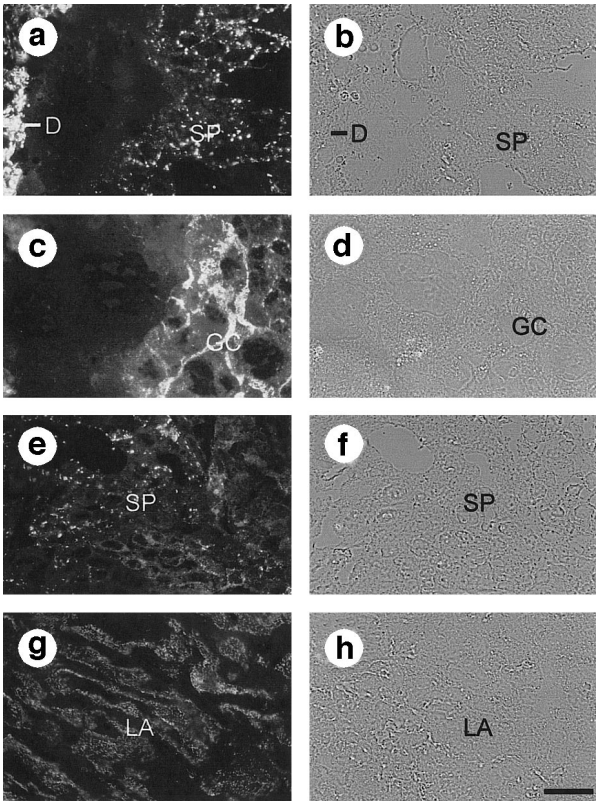

FIG. 7. Connexin expression in placenta at ED 13.5. Immunofluorescence (a, c, e, g) and corresponding phase-contrast images (b, d, f, h) of wild type placenta sections using antibodies specific to Cx43 (a–d), Cx31 (e, f), and Cx26 (g, h). Whereas Cx43 and Cx31 are coexpressed in spongiotrophoblast cells (a, e), Cx26 was restricted to the labyrinth (g). Cx43 was additionally expressed in decidua (a) and trophoblastic giant cells (c). SP, spongiotrophoblast; D, decidua; LA, labyrinth; GC, trophoblastic giant cells. Bar: 60 μm.

ectoplacental cone. Further in gestation, trophoblast cells continue to proliferate and form the labyrinth and spongiotrophoblast that, in turn, give rise to terminally differentiated giant cells. The latter become polyploid and fulfill critical functions in remodeling of maternal decidua and hormonal regulation of maternal and embryonic development. In addition, giant cells invade the maternal sinosoides.

In early placenta development of *Gjb3*$^{-/-}$ embryos, the ratio between chorionic plate stem cells, labyrinth cells, and spongiotrophoblast cells to giant cells was shifted to giant cells, suggesting that the balance between spongiotrophoblast and giant cell differentiation was disturbed. The equilibrium between proliferation and terminal differentiation of spongiotrophoblast cells is antagonistically regulated by two transcription factors of the basic helix-loop-helix family, Mash-2 and Hand-1. Mash-2 is required for spongiotrophoblast growth, while Hand-1 suppresses Mash-2 function and allows giant cell differentiation (Scott *et al.*, 2000). Mash-2-deficient mice (*mash-2*$^{-/-}$) show striking phenotypic similarities with Cx31-deficient mice. For example, placentas were normal up to ED 7.5 but did not give rise to a spongiotrophoblast and only to a rudimentary labyrinth by ED 9.5. At the border to the maternal decidua, a thick layer of secondary giant cells was observed (Guillemot *et al.*, 1994). In contrast to *Gjb3*$^{-/-}$ embryos, *mash-2*$^{-/-}$ placentas did not recover after ED 9.5 and all embryos died by ED 10.5. This was most likely the result of placental failure, because the time of embryo loss correlated with establishment of the chorio-allantoic circulation and could be overcome by aggregation of *mash-2*$^{-/-}$ embryos with tetraploid wild type embryos, which contribute only to extraembryonic tissues (Guillemot *et al.*, 1994).

Histological analyses of placentas around ED 9 suggest that placental failure is also the likely cause of *Gjb3*$^{-/-}$ embryo loss, once nutrition of the embryo relies on the chorion-allantoic placenta. The large number of giant cells found at the border between embryonic and maternal layers, the reduced labyrinth layer, and the less-frequent maternal lacunas should prevent most exchange of nutrients between mother and embryo. The transient nature of placental dysmorphogenesis could most easily be explained with compensation by other connexin isoforms expressed in the affected cell population. This could be Cx43 encoded by *Gja1*, which is strongly upregulated concomitantly with recovery of Cx31-deficient placentas. The exact time point of the upregulation of Cx43 or other, yet unidentified connexin isoforms should be critical for the rescue of *Gjb3*$^{-/-}$ embryos. Slight variations, possibly resulting from factors in the (mixed) genetic background of the mice, might be responsible for partial survival of the litters. The normal size of surviving *Gjb3*$^{-/-}$ embryos, despite the reduced placental weight, is in accordance with findings by Kurz *et al.* (1999), that there is no strict correlation between placenta size and fetal growth rate.

Reduced female fertility resulting from failure in placental development was not reported for humans that carry either recessive (Liu *et al.*, 2000) or dominant mutations (Xia *et al.*, 1998; Richard *et al.*, 1998a) in *GJB3*. This difference is most probably the result of expression of Cx40 instead of Cx31 in the corresponding physiological cell population of the extravillous trophoblast in the human placenta (Winterhager *et al.*, 1999).

The similarity between the phenotypic defects of *Gjb3*$^{-/-}$ and *mash-2*$^{-/-}$ mice prompts speculations about involvement of Cx31 and Mash-2 in the same signaling pathway. At present, however, it is difficult to predict how both proteins could interact. For Mash-2, it was shown that it acts cell-autonomously in spongiotrophoblast differentiation. Thus, in aggregation chimera, Mash-2-deficient cells could not contribute to spongiotrophoblast (Tanaka *et al.*, 1997). Mash-2 could directly or indirectly induce Cx31 expression in spongiotrophoblast precursor cells and Cx31-mediated intercellular communication could mediate the reception of proliferative signals by neighboring cells. This would place Cx31 downstream of Mash-2, which is consis-

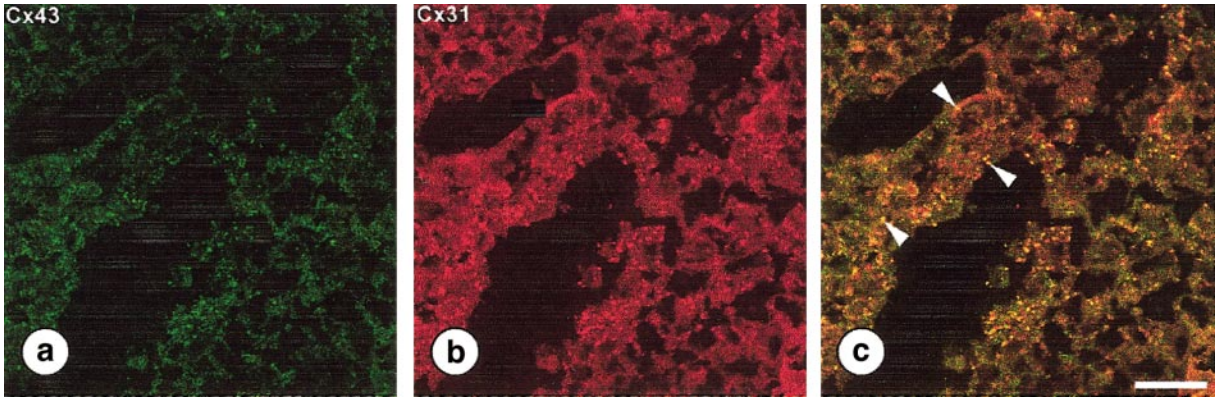

FIG. 8. Double immunofluorescents staining for Cx43 (green) and Cx31 (red) in sections of wild type placentas at ED 12.5 analyzed by confocal laser scanning microscopy. Stainings for Cx43 (a) and Cx31 (b) show that both connexin isoforms are expressed in the spongiotrophoblast layer of placenta. In the dual-scanning mode (c) the colocalization of both connexins in the same cells and even the same gap junction plaque (arrows) becomes apparent. Bar: 30 μm.

tent with the function of this transcription factor; the overlapping expression pattern in preimplantation embryos, ectoplacental cone, and spongiotrophoblast (Guillemot *et al.*, 1994; Nakayama *et al.*, 1997; Rossant *et al.*, 1998); and multiple potential binding sites for Mash-2/E-factor dimers (Johnson *et al.*, 1992) within the proximal promoter and the intron of the Cx31 gene (Plum *et al.*, in preparation).

According to an alternative hypothesis, Cx31 could act upstream of Mash-2 by mediating the intercellular exchange of low-molecular-weight messengers via gap junctional intercellular communication that could induce directly or indirectly the expression of *mash-2*.

By *lacZ*-staining of *Gjb3*$^{+/-}$ embryos, we confirmed the complex spatial and temporal pattern of expression in the embryo *proper* that overlapped with the expression of *krox-20* as previously described by Dahl *et al.* (1997). Krox-20, a zinc-finger transcription factor, is essential for hindbrain patterning, in that *krox-20*$^{-/-}$ mice exhibit a marked size decrease or elimination of rhombomeres r3 and r5, respectively (Schneider-Maunoury *et al.*, 1993). In chick, microinjection of fluorescent dyes in the developing hindbrain demonstrated not only that rhombomeres formed developmental compartments but also that gap junctional

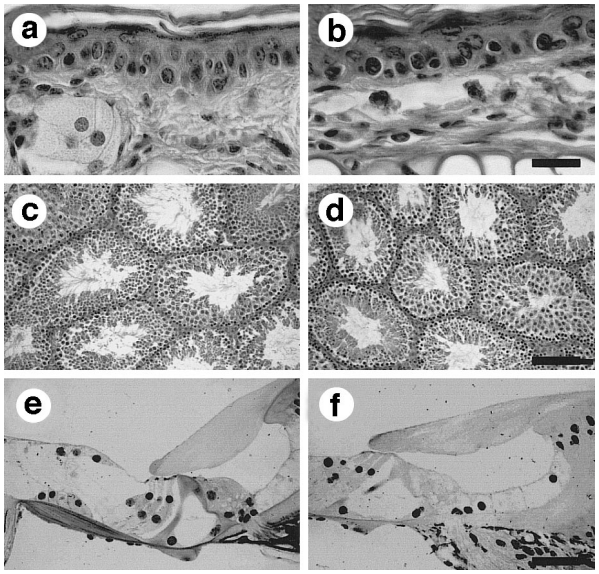

FIG. 9. Histology of adult organs of *Gjb3*$^{+/+}$ and *Gjb3*$^{-/-}$ mice. Hematoxilin and eosin stained paraffin sections of adult skin (a, b), testis (c, d), and the organ of Corti (e, f) of adult *Gjb3*$^{+/+}$ (a, c, e) and *Gjb3*$^{-/-}$ mice (b, d, f). No histological differences were observed between Cx31-deficient mice and wild type controls. Bars: 30 μm in (a, b); 150 μm in (c, d); 120 μm in (e, f).

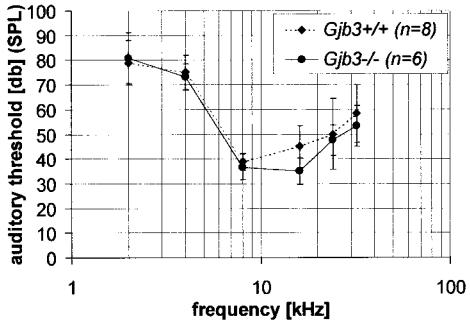

FIG. 10. Auditory thresholds of *Gjb3*$^{+/+}$ and *Gjb3*$^{-/-}$ mice. Brain stem potentials evoked by tones of various frequencies between 2 and 32 kHz and sound pressure levels (SPL) up to 100 db were recorded to determine the auditory thresholds of mutant and wild type mice. All values are presented as means ± SD. No significant differences were observed between mice of both genotypes.

intercellular communication was particular strong within rhombomeres but reduced at borders between rhombomeres (Martinez *et al.*, 1992). This could be achieved by expression of different connexin isoforms that form incompatible hemichannels in neighboring rhombomeres. Because of its incompatibility with all other connexins tested and its pattern of expression, Cx31 could mediate a similar pattern of coupling in the mouse hindbrain and thus contribute to Krox-20-mediated pattern formation. Nevertheless, we did not observe any differences in hindbrain patterning of *Gjb3*$^{-/-}$ embryos compared to that of wild type controls. In contrast to *krox-20*$^{-/-}$ mice, neither *lacZ* staining of embryos between early ED 8 and ED 11.5 differed in *Gjb3*$^{-/-}$ animals and heterozygously mutated controls, nor was the relative position of the facial/acoustic ganglia complex and the trigeminal ganglion altered in *Gjb3*$^{-/-}$ embryos at ED 11, suggesting a normal hindbrain architecture. We conclude that Cx31 is dispensable for rhombomere formation in mice.

Despite mutations in human *GJB3* that were reported to be causal to the inherited skin disorder *erythrokeratodermia variabilis* (Richard *et al.*, 1998a) and hearing impairments (Xia *et al.*, 1998; Liu *et al.*, 2000), respectively, no morphological defects were found in skin or inner ear of *Gjb3*$^{-/-}$ mice and audiometry of *Gjb3*$^{-/-}$ mice did not reveal any functional hearing impairment. This discrepancy could be explained either by differences in the expression of connexin isoforms, differences in the physiology of the affected organs, or by the type of mutation. Thus, single-base mutations found in patients with *erythrokeratodermia variabilis* could lead to dominant negative acting Cx31 mutants that are able to inhibit not only wild type Cx31 protein but also other connexin isoforms expressed in the same cell type and, consequently, have a more severe impact on gap junctional intercellular communication than the mere absence of Cx31 in *Gjb3*$^{-/-}$ mice.

The same argument might hold true for dominant mutations in the human Cx31 gene, causing high-frequency hearing impairment. Interestingly, *trans*-dominant acting mutations in human Cx26 and Cx30 genes, leading to deafness in combination with another genodermatose, keratoderma palmoplantar, and nonsyndromic deafness, respectively, were previously described (Richard *et al.*, 1998b; Grifa *et al.*, 1999). However, a recent report that associated recessive mutations in human *GJB3* with nonsyndromic deafness (Liu *et al.*, 2000) pointed to a more direct involvement of Cx31 in human hearing that cannot be mimicked in Cx31-deficient mice. Thus, differences in expression or function of connexin isoforms in the inner ear of humans and mice may exist. Using *lacZ* staining and immunofluorescence, we could not detect Cx31 expression in the adult inner ear of mice and rat (Lautermann *et al.*, 1998). Furthermore, Northern blot analysis did detect transcripts of the Cx26 and Cx30 but not of the Cx31 gene in total RNA of rat inner ear (Winterhager and Lautermann, unpublished results).

Nevertheless, Xia and Coworkers (1998) detected Cx31 transcript in the inner ear of rats, using reverse transcription PCR, and recently Cx31 protein was described by Xia *et al.* (2000) to be expressed in a basal-to-apical gradient in the spiral ligament of the cochlea using immunohistochemistry. While the detection of Cx31 transcript by RT-PCR in these studies could most easily be explained by the expression of Cx31 in tissues adjacent to the cochlea, the contradictory results regarding Cx31 protein expression are most likely based on methodological differences. Xia and coworkers used commercially available antibodies directed to Cx31, whereas we used Cx31 antibodies previously characterized in our group (Butterweck *et al.*, 1994). Thus, the immunoreactivity seen by Xia *et al.* (2000) could be due to cross-reactivity of their antibodies with a not yet identified connexin isoform. This could most easily be checked by repeating the experiment using various tissues that are known to express Cx31 as positive controls and Cx31-deficient cochleae from *Gjb3*$^{-/-}$ mice as negative controls.

In conclusion, Cx31 is essential for cell differentiation during early stages of placental development. Later in development its loss can be functionally compensated, leading to normal placentas at term. Cx43, which is upregulated in Cx31-expressing spongiotrophoblast cells with ongoing development, could compensate for the loss of Cx31, leading to a resumption of placenta differentiation and growth. This hypothesis could be tested most directly by the analysis of mice that are deficient for both isoforms, Cx31 and Cx43. Comparison of *Gjb3*$^{-/-}$ and *mash-2*$^{-/-}$ embryos could help to understand whether both proteins act in the same signal transduction pathway that controls the decision between spongiotrophoblast proliferation and giant cell differentiation. Provided a role of gap junctional intercellular communication in morphogenesis and physiology of adult organs, the lack of obvious defects in Cx31-deficient embryos as well as in adult skin and ear suggests a high degree of functional redundancy among members of the connexin gene family. Thus, to reveal the role(s) of direct intercellular communication, coupling might have to be reduced further. This could be achieved by combining multiple connexin null alleles in one mouse line or, more elegantly, by *trans*-dominant-negative connexin mutants inducibly expressed as a transgene in the tissue of interest.

ACKNOWLEDGMENTS

We thank Dr. Frank Sablitzky (London, UK) for the vector pLRlacZpAMCIneopA, Drs. Eberhard Wenzel and Susanne Dubiel for help with establishment of brain stem audiometry, and Georgia Rauter for technical assistance. This work was supported by grants of the Dr. Mildred Scheel Stiftung, the Thyssen Stiftung, the Deutsche Forschungsgemeinschaft, and the Fonds der Chemischen Industrie to K.W.

REFERENCES

Ausubel, F. M., Brent, R., Kingston, R. E., Moore, D. D., Seidmann, J. G., Smith, J. A., and Struhl, K. (1989). "Current Protocols in Molecular Biology." Wiley, New York.

Butterweck, A., Elfgang, C., Willecke, K., and Traub, O. (1994). Differential expression of the gap junction proteins connexin45, -43, -40, -31, and -26 in mouse skin. *Eur. J. Cell Biol.* **65,** 152–163.

Dahl, E., Willecke, K., and Balling, R. (1997). Segment-specific expression of a gap junction gene, connexin31, during hindbrain development. *Dev. Genes Evol.* **207,** 359–361.

Dahl, E., Winterhager, E., Reuss, B., Traub, O., Butterweck, A., and Willecke, K. (1996). Expression of the gap junction proteins connexin31 and connexin43 correlates with communication compartments in extraembryonic tissues and in the gastrulating mouse embryo, respectively. *J. Cell Sci.* **109,** 191–197.

Davies, T. C., Barr, K. J., Jones, D. H., Zhu, D. G., and Kidder, G. M. (1996). Multiple members of the connexin gene family participate in preimplantation development of the mouse. *Dev. Genet.* **18,** 234–243.

Elfgang, C., Eckert, R., Lichtenberg-Fraté, H., Butterweck, A., Traub, O., Klein, R. A., Hülser, D., and Willecke, K. (1995). Specific permeability and selective formation of gap junction channels in connexin-transfected HeLa cells. *J. Cell Biol.* **129,** 805–817.

Goodenough, D. A., Golliger, J. A., and Paul, D. L. (1996). Connexins, connexons and intercellular communication. *Annu. Rev. Biochem.* **65,** 475–502.

Grifa, J., Wagner, D'Ambrosio, C. A., Melchionda, L., Bernardi, S., Lopez-Bigas, F., Rabionet, N., Arbones, R., Della Monica, M., Estivill, X., Zelante, L., Lang, F., and Gasparini, P. (1999). Mutations in gjb6 cause nonsyndromic austosomal dominant deafness at DFNA3 locus. *Nat. Genet.* **23,** 16–18.

Grummer, R., Hellmann, P., Traub, O., Soares, M. J., and Winterhager, E. (1996). Regulation of connexin31 gene expression upon retinoic acid treatment in rat choriocarcinoma cells. *Exp. Cell Res.* **227,** 23–32.

Guillemot, F., Nagy, A., Auerbach, A., Rossant, J., and Joyner, A. L. (1994). Essential role of Mash-2 in extraembryonic development. *Nature* **371,** 333–336.

Hennemann, H., Schwarz, H. J., and Willecke, K. (1992). Characterization of gap junction genes expressed in F9 embryonic carcinoma cells: Molecular cloning of mouse connexin31 and -45 cDNAs. *Eur. J. Cell Biol.* **57,** 54–58.

Hogan, B., Beddington, R., Constantini, F., and Lacey, E. (1994). "Manipulating the Mouse Embryo: A Laboratory Manual." CSHL Press, New York.

Johnson, J. E., Birren, S. J., Saito, T., and Anderson, D. J. (1992). DNA binding and transcriptional regulatory activity of mammalian achaete-scute homologous (MASH) proteins revealed by interaction with a muscle-specific enhancer. *Proc. Natl. Acad. Sci. USA* **89,** 3596–3600.

Kunzelmann, P., Schröder, W., Traub, O., Steinhäuser, C., Dermietzel, R., and Willecke, K. (1999). Late onset and increasing expression of the gap junction protein connexin30 in adult murine brain and longterm cultured astrocytes. *Glia* **25,** 111–119.

Kurz, H., Zechner, U., Orth, A., and Fundele, R. (1999). Lack of correlation between placenta and offspring size in mouse interspecific crosses. *Anat. Embryol. (Berl.)* **200,** 335–343.

Lautermann, J., Ten, C. W., Altenhoff, P., Grummer, R., Traub, O., Frank, H., Jahnke, K., and Winterhager, E. (1998). Expression of the gap-junction connexins 26 and 30 in the rat cochlea. *Cell Tissue Res.* **294,** 415–420.

Liu, X. Z., Xia, X. J., Xu, L. R., Pandya, A., Liang, C. Y., Blanton, S. H., Brown, S. D., Steel, K. P., and Nance, W. E. (2000). Mutations in connexin31 underlie recessive as well as dominant non-syndromic hearing loss. *Hum. Mol. Genet.* **9,** 63–67.

Manthey, D., Bukauskas, F., Lee, C. G., Kozak, C. A., and Willecke, K. (1999). Molecular cloning and functional expression of the mouse gap junction gene connexin-57 in human HeLa cells. *J. Biol. Chem.* **274,** 14716–14723.

Martinez, S., Geijo, E., Sanchez, V. M., Puelles, L., and Gallego, R. (1992). Reduced junctional permeability at interrhombomeric boundaries. *Development* **116,** 1069–1076.

Moll, R., Franke, W. W., Schiller, D. L., Geiger, B., and Krepler, R. (1982). The catalog of human cytokeratins: Patterns of expression in normal epithelia, tumors and cultured cells. *Cell* **31,** 11–24.

Nagy, A., Rossant, J., Nagy, R., Abramow-Newerly, W., and Roder, J. C. (1993). Derivation of completely cell culture-derived mice from early-passage embryonic stem cells. *Proc. Natl. Acad. Sci. USA* **90,** 8424–8428.

Nakayama, H., Liu, Y., Stifani, S., and Cross, J. C. (1997). Developmental restriction of Mash-2 expression in trophoblast correlates with potential activation of the notch-2 pathway. *Dev. Genet.* **21,** 21–30.

Reuss, B., Hellmann, P., Dahl, E., Traub, O., Butterweck, A., Grummer, R., and Winterhager, E. (1996). Connexins and E-cadherin are differentially expressed during trophoblast invasion and placenta differentiation in the rat. *Dev. Dyn.* **205,** 172–182.

Richard, G., Smith, L. E., Bailey, R. A., Itin, P., Hohl, D., Epstein, E. H., Jr., DiGiovanna, J. J., Compton, J. G., and Bale, S. J. (1998a). Mutations in the human connexin gene GJB3 cause erythrokeratodermia variabilis. *Nat. Genet.* **20,** 366–369.

Richard, G., White, T. W., Smith, L. E., Bailey, R. A., Compton, J. G., Paul, D. L., and Bale, L. J. (1998b). Functional defects of Cx26 resulting from a heterozygous missense mutation in a family with dominant deaf-mutism and palmoplantar keratoderma. *Hum. Genet.* **103,** 393–399.

Rossant, J., Guillemot, F., Tanaka, M., Latham, M., Gertenstein, M., and Nagy, A. (1998). Mash2 is expressed in oogenesis and preimplantation development but is not required for blastocyst formation. *Mech. Dev.* **73,** 183–191.

Schneider-Maunoury, S., Topilko, P., Seitandou, T., Levi, G., Cohen-Tannoudji, M., Pournin, S., Babinet, C., and Charnay, P. (1993). Disruption of Krox-20 results in alteration of rhombomeres 3 and 5 in the developing hindbrain. *Cell* **75,** 1199–1214.

Scott, I. C., Anson-Cartwright, L., Riley, P., Reda, D., and Cross, J. C. (2000). The HAND1 basic helix-loop-helix transcription factor regulates trophoblast differentiation via multiple mechanisms. *Mol. Cell Biol.* **20,** 530–541.

Sonnenberg, A., Calafat, J., Janssen, H., Daams, H., Raaij-Helmer, L. M., Falcioni, R., Kennel, S. J., Aplin, J. D., Baker, J., and Loizidou, M. (1991). Integrin alpha 6/beta 4 complex is located in hemidesmosomes, suggesting a major role in epidermal cell-basement membrane adhesion. *J. Cell Biol.* **113,** 907–917.

Steel, K. P. (1998). One connexin, two diseases. *Nat. Genet.* **20,** 319–320.

Steel, K. P., and Bussoli, T. J. (1999). Deafness genes: Expressions of surprise. *Trends Genet.* **15,** 207–211.

Tanaka, M., Gertsenstein, M., Rossant, J., and Nagy, A. (1997). Mash2 acts cell autonomously in mouse spongiotrophoblast development. *Dev. Biol.* **190,** 55–65.

Traub, O., Eckert, R., Lichtenberg-Fraté, H., Elfgang, C., Bastide, B., Scheidtmann, K. H., Hülser, D. F., and Willecke, K. (1994). Immunochemical and electrophysiological characterization of

murine connexin40 and -43 in mouse tissues and transfected human cells. *Eur. J. Cell Biol.* **64,** 101–112.

Traub, O., Look, J., Dermietzel, R., Brummer, F., Hülser, D., and Willecke, K. (1989). Comparative characterization of the 21-kD and 26-kD gap junction proteins in murine liver and cultured hepatocytes. *J. Cell Biol.* **108,** 1039–1051.

Winterhager, E., Reuss, B., Hellmann, P., Spray, D. C., and Gruemmer, R. (1996). Gap junction and tissue invasion: A comparison of tumorigenesis and pregnancy. *Clin. Exp. Pharmacol. Physiol.* **23,** 1058–1061.

Winterhager, E., Von Ostau, C., Gerke, M., Gruemmer, R., Traub, O., and Kaufmann, P. (1999). Connexin expression patterns in human trophoblast cells during placental development. *Placenta* **20,** 627–638.

Xia, A.-P., Ikeda, K., Katori, Y., Oshima, T., Kikuchi, T., and Takasaka, T. (2000). Expression of connexin31 in the developing mouse cochlea. *Neuroreport* **11,** 2449–2453.

Xia, J. H., Liu, C. Y., Tang, B. S., Pan, Q., Huang, L., Dai, H. P., Zhang, B. R., Xie, W., Hu, D. X., Zheng, D., Shi, X. L., Wang, D. A., Xia, K., Yu, K. P., Liao, X. D., Feng, Y., Yang, Y. F., Xiao, Y. J., Xie, D. H., and Huang, J. Z. (1998). Mutations in the gene encoding gap junction protein beta-3 associated with autosomal dominant hearing impairment. *Nat. Genet.* **20,** 370–373.

Received for publication May 10, 2000
Revised November 16, 2000
Accepted December 22, 2000
Published online February 9, 2001